In situ temperature programmed desorption of Ⅲ-nitride photocathode

Cheng Wei[1,2], Shi Feng[1,2], Yang Shuning[1,2], Zhou Yujian[1,2], Ren Bin[1,2],

(1. Science and Technology on Low-Light-Level Night Vision Laboratory, Xi′an 710065, China;
2. Kunming Institute of Physics, Kunming 650223, China)

Abstract: Theoretical thermal desorption and in situ temperature programmed desorption (TPD) were developed to study the degassing of contaminants adsorbed in Ⅲ-nitride photocathodes assembly. In the frame of Malev′ sadsorption-diffusion outgassing theory, one dimensional slab was used to model the photocathodes assembly. By using the first and the second Fick′ slaw, the expressions of the special gas concentration, the specific gas outgassing rate and the amount of degased specific gas over the time in the degassing process were obtained. To make it more intuitional, these parameters were ploted over time within different diffusion coefficient magnitude at the approximation of fourth order. In the TPD method for Ⅲ-nitride photocathodes assembly, residual gas mass spectrum was thoroughly studiedat different constant temperature stage to determine which gases were desorbed into the vacuum. The least square method was employed to fit the expression of the specific outgassing rate at the constant temperature of 1 000 K, and the diffusion coefficient D for outgassing N_2 was 5×10^{-5} cm^2/s in the dynamic method of degassing process. By combining theoretical analysis with TPD experiments, the heating up temperature for sufficient outgassing the contaminants from the Ⅲ-nitride photocathodes assembly was evaluated and verified.

Key words: Ⅲ-nitride photocathode assembly; temperature programmed desorption; residual gas spectrum

CLC number: TN216 **Document code:** A DOI: 10.3788/IRLA201948.1017002

Ⅲ族氮化物光电阴极原位程序升温脱附

成 伟[1,2],石 峰[1,2],杨书宁[1,2],周玉鉴[1,2],任 彬[1,2]

(1. 微光夜视技术重点实验室,陕西 西安 710065; 2. 昆明物理研究所,云南 昆明 650223)

摘 要: 建立了理论热脱附和原位程序升温脱附方法研究 III 族氮化物光电阴极部件的热除气过程。基于 Malev 吸附-扩散除气理论搭建了光电阴极的平板模型，利用 Fick 第一和第二定理计算得到了除气过程中样品吸附气体浓度、瞬时除气速率以及总的气体脱附量随时间变化的表达式。为便于直观研究,通过截取四阶近似给出不同扩散系数量级下的以上参量随时间的变化曲线。在 III 族氮化物光

收稿日期: 2019-06-08; **修订日期:** 2019-07-14

基金项目: 国防预先研究基金(9140C380502150C38002)

作者简介: 成伟(1977-),男,高级工程师,硕士,主要从事半导体器件测试方面的研究。Email:szray@21cn.com

通讯作者: 任彬(1981-),男,高级工程师,博士,主要从事微光像增强器方面的研究。Email:robinson_cv@163.com

电阴极 TPD 动态法实验中，研究并分析了光电阴极部件在不同恒温除气阶段的残余气体谱图，由此得出进入真空中的脱附气体种类。采用最小二乘法拟合得到：恒温 1 000 K 的条件下，N_2 的扩散系数为 5×10^{-5} cm^2/s。通过理论分析结合 TPD 实验，III 族氮化物光电阴极部件热清洗的有效去除污染加热温度得到了有效的评估和验证。

关键词：III 族氮化物光电阴极部件； 程序升温脱附； 残余气体谱

0 Introduction

UV photocathode as a core component of the UV converter tube, has been widely used in astronomy science, UV detection and electron emission systems. III−nitride photocathode, which can be modulated for the response wavelength even to solar blind region, has much superiority to the other UV photocathodes, such as Cs_2Te, CsI, et al[1−2].

Surface contamination is a major factor influencing the operation of UV photocathodes. Tracing inorganic or organic contaminations have been shown to have a detrimental impact on photocathode performance and quantum yield. After the photocathodes wafer is transferred from the MBE or MOCVD equipment to the air circumstance, variety contaminations begins. Photocathodes wafer may adsorb gases from box under storage, shipment, and preparing process. The amount of contaminations results in the wafer surface depending on the temperature pressure, and the duration time of exposure[3].

When a photocathode wafer is loaded into an ultra-high vacuum (UHV) chamber, it will give off the absorbed gases spontaneously. Usually, we can accumulate this process by heating up the sample, this technology is called heating up outgassing to achieve an atom-level clean surface. In addition, in the manufacture process of image intensifier assembly, not only the photocathode, but also the other components, such as the MCP, the envelop of the tube, and the phosphor should be outgassed thoroughly [4]. Of course, the outgassing of the photocathode is not only related to its properties, but also to the circumstance under storage, shipment, manufacture process and other factors, similar to the adsorption process.

This paper describes the theoretical and experimental investigation of the outgassing for III−nitride photocathode assembly, the instant quantity of specific outgassing gases of components are analyzed. Then, the gradient of its parameters in the diffusion model is fitted to characterize it.

1 Ⅲ−nitride photocathode structure

Figure 1 shows the schematic of cross section of a III−nitride photocathode assembly. The substrate of basal plane (0001) sapphire is double-side-polished to allow for the realization of semi-transparent photocathode. A low-temperature nucleation layer AlN was first grown on 5 μm diameter substrate, followed by 0.3 μm high-temperature buffer layer AlN. The top film of 0.1 μm thickness P−AlGaN is the optical-electronic convertion layer.

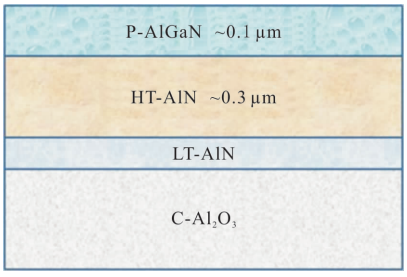

Fig.1 Schematic of cross section of a III−nitride photocathode assembly

After the growth was completed, the wafer of the III−nitride photocathode structure is cut into ~18 mm small piece to carry out the experiments, the subsequent process is similar with the GaAs photocathode preparation[5].

2 Theoretical desorption of the III-nitride photocathode

2.1 Material degassing theory

Any solid material would bleed gas in vacuum because of dissolving[6]. In order to quantify the amount of outgassing from the photocathode assembly, models for outgassing from the adsorption on photocathode surfaces should be established firstly. Theoretical behavior of the total outgassing was modeled based on published solution of the diffusion equation founded in the literature. One of the outgassing model of Malev theory has been widely used[7], which considered both surfaces and volume process based on two assumptions: (1) metal and gas interacting speed was much faster than diffusion velocity so that the balance time of adsorbing gas in the metal could be ignored; (2) solid adsorbing gas and outgassing are in equilibrium state.

In Malev theory, the released gas from sample can be divided into two steps, first is the gas diffusion in the material; second is related to the desorption of adsorbing gas from the surface. This model of outgassing is often called "adsorption-diffusion model", it could be described by the first and the second Fick law: gas diffusion coefficient that passed unit area in unit time has relation with gas concentration gradient.

2.2 Behavior of the theoretical degassing process

The outgassing of the III-nitride photocathode assembly can be modeled by a slab in the vacuum, as illustrated in Fig.2.

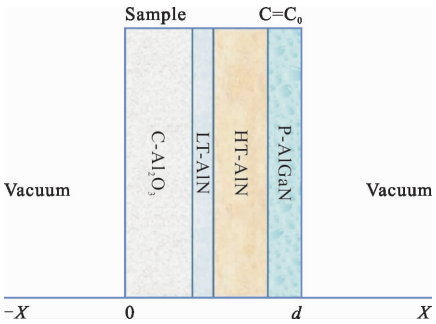

Fig.2 Schematic diagram of one dimensional sample and boundary conditions for outgassing

The diffusion equation is given by:

$$\frac{\partial C}{\partial t}=D\frac{\partial^2 C}{\partial^2 x'} \tag{1}$$

and the boundary conditions are as belows:

$$C=C_0 \quad t=0;\ 0<x<d$$
$$C=0 \quad t>0;\ x=0$$
$$C=0 \quad t>0;\ x=d$$

where C_0 is the initial gas concentration in the sample, in moleculers/cm^3; D is the diffusion coefficient, in cm^2/s; C is the gas concentration, and d is the thickness of the sample, in cm. Using separation of variables method to solve Eq. (1) restrained in the boundary conditions, the gas concentration C is obtained as:

$$C=f(x,t)=C_0\frac{4}{\pi}\sum_0^{\infty}(2n+1)^{-1}\sin\frac{\pi(2n+1)x}{d}\cdot \exp\left\{-\left[\frac{\pi(2n+1)x}{d}\right]^2 Dt\right\} \tag{2}$$

Once the diffusion coefficient D is given, the kinetics of outgassing with initial gas concentration C_0 can be confirmed. The relationship between diffusion coefficient D and temperature T can be expressed with Arrhenius equation[8]:

$$D=D_0\exp\left(\frac{E_A}{kT}\right) \tag{3}$$

D_0 is the pre-exponential coefficient, in cm^2/s; and E_A is the desorption activation energy, in J/mol; T is the absolute temperature. Specific outgassing rate q can be obtained using Fick′s law by setting $x=0$ at the surface, in molecules/(cm^2·s):

$$q=2D\left(\frac{\partial C}{\partial x}\right)_{x=0}=\frac{8C_0D}{d}\cdot \sum_0^{\infty}\exp\left\{-\left[\frac{\pi(2n+1)}{d}\right]^2 Dt\right\} \tag{4}$$

From the definition, q is directly proportional to the instant quantity of special gas, and can be rewritten as:

$$\frac{qd}{8C_0}=2D\left(\frac{\partial C}{\partial x}\right)_{x=0}=D\cdot\sum_0^{\infty}\exp\left\{-\left[\frac{\pi(2n+1)}{d}\right]^2 Dt\right\} \tag{5}$$

For simplicity, we define x/d as $x_1\in[0,1]$, Dt/d^2 as x_2, and Eq.(2) can be written as:

$$\frac{C}{C_0}=\frac{4}{\pi}\sum_0^{\infty}(2n+1)^{-1}\sin\pi(2n+1)x_1\cdot\exp\{-[\pi(2n+1)]^2x_2\} \tag{6}$$

At time t, the amount of specific outgassing gas Q, which means the total quantity of specific outgassing gas is given by:

$$Q=\int_0^t q\mathrm{d}t=\frac{8C_0d}{\pi^2}\{\sum_0^{\infty}\frac{1}{(2n+1)^2}\cdot\left[1-\exp\left(-Dt\cdot\left(\frac{\pi(2n+1)}{d}\right)^2\right)\right]\} \tag{7}$$

Equation (7) can be rewritten as:

$$\frac{Q\pi^2}{8C_0d}=\sum_0^{\infty}\frac{1}{(2n+1)^2}\left[1-\exp\left(-Dt\cdot\left(\frac{\pi(2n+1)}{d}\right)^2\right)\right] \tag{8}$$

We consider the approximation of forth order, as we set $n=4$, and plug $d=0.05$ cm into the Eqs. (6), (8) and (5), then we obtain:

$$\frac{C}{C_{0n=4}}=\frac{\sin(\pi\cdot x_1)}{\sin(\pi^2\cdot x_2)}+\frac{\sin(3\pi\cdot x_1)}{3\sin(9\pi^2\cdot x_2)}+\frac{\sin(5\pi\cdot x_1)}{5\sin(25\pi^2\cdot x_2)}+\frac{\sin(7\pi\cdot x_1)}{7\sin(49\pi^2\cdot x_2)}+\frac{\sin(9\pi\cdot x_1)}{9\sin(81\pi^2\cdot x_2)} \tag{9}$$

$$\frac{Q\pi^2}{8C_0d_{n=4}}=\sum_0^{\infty}\frac{1}{(2n+1)^2}\left[1-\exp\left(-Dt\cdot\left(\frac{\pi(2n+1)}{d}\right)^2\right)\right]=\frac{117\,469}{99\,225}-\frac{1}{\exp\left(\frac{D\pi^2t}{d^2}\right)}-\frac{1}{9\exp\left(\frac{9D\pi^2t}{d^2}\right)}-\frac{1}{25\exp\left(\frac{25D\pi^2t}{d^2}\right)}-\frac{1}{49\exp\left(\frac{49D\pi^2t}{d^2}\right)}-\frac{1}{81\exp\left(\frac{81D\pi^2t}{d^2}\right)} \tag{10}$$

$$\frac{qd}{8C_{0n=4}}=\frac{D}{\exp(400D\pi^2t)}+\frac{D}{\exp(3\,600D\pi^2t)}+\frac{D}{\exp(10\,000D\pi^2t)}+\frac{D}{\exp(19\,600D\pi^2t)}+\frac{D}{\exp(32\,400D\pi^2t)} \tag{11}$$

Figure 3 is the theoretical heating outgassing desorption curves calculated from Eqs. (9), (10) and (11). Figure 3 (a) is the relative specific gas concentration C changed over time. The gas concentration changes from up to down, accompanied by x increasing from $C1$ to $C6$. We can conclude, after the sample of III-nitride photocathode is loaded into the UHV chamber, the adsorbed gas at the surface could desorb quickly and pumped away, leaving the adsorption sites at the surface. Then, under the driven potential generated by the gradient of concentration between the surface and the middle of the slab, the solute gas in the bulk near the surface begins to migrate to the surface, again desorbs and pumps away. Over time, the gas concentration in the middle of the slab begins to decrease at last. But when the diffusion coefficient D is small, it takes too long time to let the gas concentration in the middle of the slab to reduce.

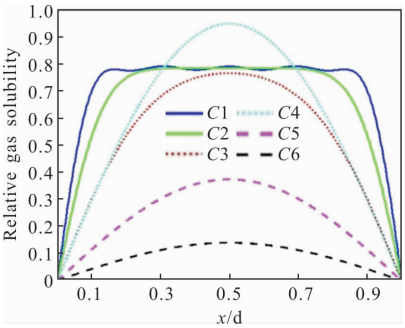

(a) Relative specific gas concentration C

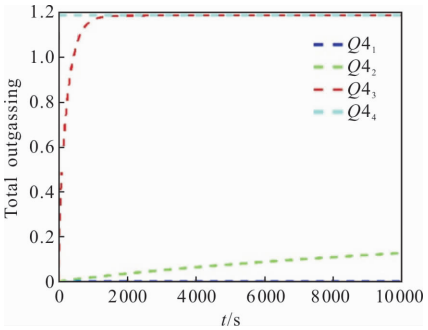

(b) Relative specific outgassing gas Q

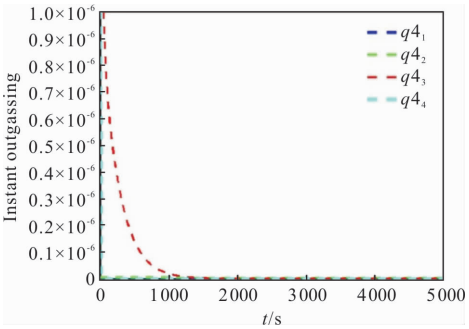

(c) Relative specific outgassing rate q

Fig.3 Theoretical heating outgassing desorption curves for the order of n=4

Considering the diffusion coefficient D is on the order of 10^{-12}, 10^{-11}, 10^{-9}, 10^{-6} cm^2/s, we plot the

relative specific outgassing gas Q changed over time in Fig.3 (b). We define when Q reduced to 1/e of its initial valve as the criterion for sufficient outgassing. From Fig.3 (b), we can see it takes 1 700 seconds for sufficient outgassing when D equals to 10^{-9} cm^2/s, while when D equals to 10^{-6} cm^2/s, it takes very soon for sufficient outgassing; and it takes very long time for D bellows 10^{-11} cm^2/s. We plug these four values of D into Eq. (11), the instant outgassing rate of special gas is obtained in Fig.3 (c). Compared with Fig.3 (b), when the total outgassing gas Q move towards saturation, the instant outgassing rate drops down quickly.

3 TPD experiments

3.1 TPD experiment design

An extensive mass-spectral analysis study demands a series of complete mass spectrum. Quadrupole mass spectrometer has found a wide range of applications in the residual gas analysis and a process monitoring devices in semiconductor fabrication plants. The equipment was mounted on vacuum flange with a VG ion source in UHV testing facility, the resolution have been improved by increasing AC operating frequency, and the electron multipliers have been used to increase sensitivity by detecting very low trace of pollutions. In the process of outgassing testing, quadrupole mass spectrometer emitting current was 200 mA, the scanning rate was 2 000 ms/amu, and mass number range was 1–80 amu.

Generally, testing methods can be divided into two types of statistic method and dynamic method. Statistic method means the measurement carried out isolated from the pumping system. Dynamic method means the measurement is not isolated from the pumping system. From the view of engineering point, the result of choosing dynamic method in exhausting is beneficial for the design of vacuum system. At the same time, the redundancy rate for the gas exhausting load is also increased, as well as the reliability of the system.

TPD method is a widely used technology in vacuum, from which we can obtain the peak temperature of degassing special gas and exhausting load in the heating process. Furthermore, the characteristics of degassing temperature and desorption activation potential for special pollutions can also be obtained. In the experiment, TPD was carried out in a UHV chamber manufactured by Austenitic stainless steels. The chamber had been baked out at 300 ℃ for 24 hours to improve the vacuum degree to 10×10^{-8} Pa.

3.2 Analysis of residual gas spectrum

As can be seen in Fig.4, the process of degassing and heat cleaning of the Ⅲ–nitride photocathode is divided into 5 stages as labeled from 1 to 5 in Fig.4(a). The initial temperature was at 300 K; the second stage was heated up to 380–420 K; the third stage was heated up to 600–650 K, the fourth stage was heated up to 910–960 K, and the fifth stage was heated up to 1 010–1 050 K, then the sample maintained at this temperature for a period of time. From the beginning of the heating to the end, the sample took about 3 hours in heating up process.

From Fig.4(b) to Fig.4(e), we can see what kind of gases exist in the vacuum environment when the sample experiences the heating process. Figure 4 (b) shows the residual gas mass spectrum in the vacuum chamber after being baked out for 24 hours, we can see there were H_2(m=2), O(m=6), H_2O(m=18), Ne(m=20), N_2(m=28), Ar(m=40). Compared with Fig.4 (c) to Fig.4 (e), the residual gas mass spectrum of Fig.4(b) was much cleaner, none of the C_xH_y contaminants with mass number greater than 45 can be seen, it also proved the effect of using oil-free pump system. In addition, we can notice that the ionization current of hydrogen and water were almost in the equivalent order.

The second stage of residual gas mass spectrum was in Fig.4(c), we can see that the ionization current of H_2, O, H_2O, N_2, and CO_2 begins to increase sharply, especially the H_2O and N_2 almost increase up to two orders of the first stage. Compared with the

Fig.4 (a), we notice that H_2, H_2O and N_2 reached its first peak separately, which means they form the physisorption or weak adsorption state at this temperature.

From the third stage of residual gas mass spectrum in Fig.4 (d), we can see the outgassing rate of all gases, such as H_2, O, H_2O, N_2, and CO_2, still maintained at the level of the second stage, but they had begun to decline. In contrast with Fig.4 (a), we also noticed that H_2 and N_2 experienced its second peak, which means they form the chemisorption or strong peak adsorption state at this temperature, while O and CO_2 form the phsisorption state at this temperature, So the desorption activation energy of O and CO_2 are higher than that of H_2 and N_2. From Fig.4(a), the ionization current of H_2O continues to be downward, which means H_2O does not exist the second adsorption state. In addition, traces of contaminants with mass number greater than 45 begin to appear, indicating the C_xH_y organic contaminations have higher desorption activation energy than the inorganic contaminations.

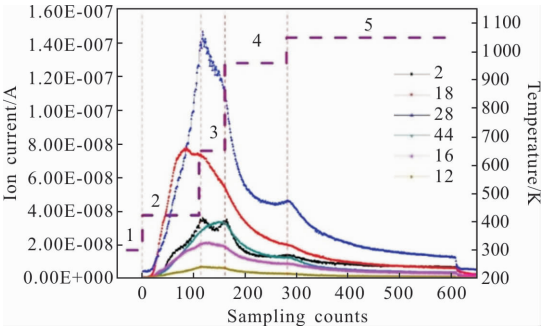

(a) Ionization currents changed over time of mass number 2, 12, 16, 18, 28 and 44, the right axis represent the temperature of stabilization stage

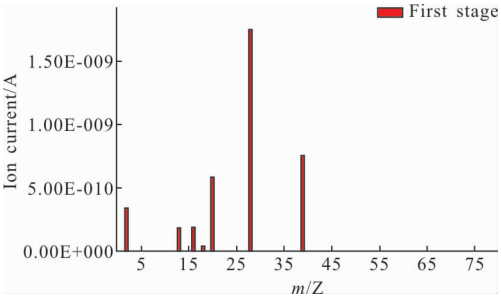

(b) Residual gas spectrum in the first stage

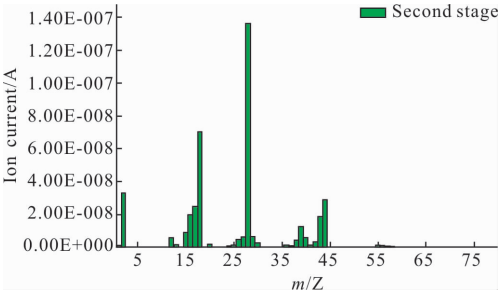

(c) Residual gas spectrum in the second stage

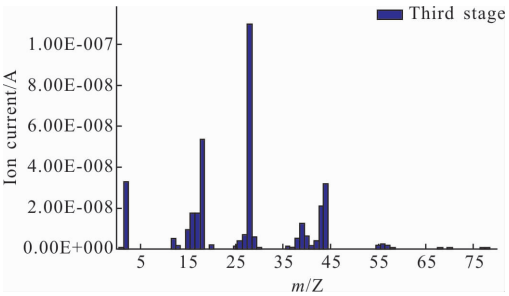

(d) Residual gas spectrum in the third stage

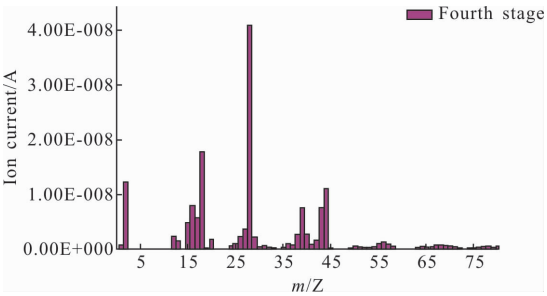

(e) Residual gas spectrum in the fourth stage

Fig.4 Residual gas mass spectrum of in situ III-nitride photocathode in temperature programmed desorption process

From the fourth stage of residual gas mass spectrum in Fig.4 (e), we can see the outgassing rate of N_2 dropped one order, and the other gases also go downward to about 1/e of the peak outgassing rate. It means the inorganic contaminations of lower mass were almost outgassed, while the outgassing rate of C_xH_y organic contaminants of higher mass were still increasing. Compared with outgassing rate of C_xH_y contaminations and other inorganic contaminations, we can conclude that the C_xH_y contaminations should be avoided as far as possible in the Ⅲ-nitride photocathode assembly preparing process, since they have high desorption activation potential, and are

hardly to remove by heating up outgassing method.

To evaluate the diffusion coefficient D in the fifth constant temperature stage from Fig.4 (a), the least square method is employed to fitting the Eq.(11), the diffusion coefficient D for outgassing N_2 in III-nitride photocathode is about 5×10^{-5} cm^2/s. Of course, the dynamic method and the non-isolated heating process will cause this value to deviate from the real value, but it has reference significance in some degree.

4 Conclusions

In this article, we report the key processing of in situ heating up for outgassing contaminations from the III-nitride photocathode assembly. Combined with the Malev′s adsorption-diffusion outgassing theory and TPD method, the expressions of the special gas concentration, the specific gas outgassing rate and the amount of specific gas over the time in the degassing process have been thoroughly analyzed, so an efficient and reasonable heating up program for outgassing of contaminants from the III-nitride photocathode assembly has been designed. The diffusion coefficient D for outgassing in 1 000 K of the III-nitride photocathode assembly is evaluated to be in the dynamic method of degassing.

We firstly studied the degassing behavior for III-nitride photocathodes assembly theoretically, it makes good sense for the preparation of III-nitride photocathode assembly to achieve atom-level clean surface before the next step of activation by low work function coatings.

Reference:

[1] Ren Bin, Shi Feng, Guo Hui, et al. First principles study on NEA GaN photocathode[J]. ***Infrared and Laser Engineering***, 2015, 44(9): 2752-2756. (in Chinese)

[2] Wang Shurong, Qu Yi, Li Futian. Study of atmospheric background and target chareacteristic in ultraviolet band[J]. ***Infrared and Laser Engineering***, 2007, 36 (s2): 433-435. (in Chinese)

[3] Dyer J S, Benson R C, Phillips T E, et al. Outgassing analyses performed during vacuum bakeout of components painted with Chemglaze Z306/9922[C]//SPIE, 1992: 177-194.

[4] Xie Yuntao, Zhang Yujun, Wang Xi, et al. Research on the gain saturation effect of an image intensifier based on microchannel plate [J]. ***Infrared and Laser Engineering***, 2017, 46(10): 1003005. (in Chinese)

[5] Ren Bin, Shi Feng, Guo Hui, et al. Cs, O adsorption for forming GaAs photocathodes [J]. ***Infrared and Laser Engineering***, 2016, 45(8): 0821001. (in Chinese)

[6] Liu Dafu, Huang Yangcheng, Wu Ligang, et al. Property analysis of window sorbate of infrared detector working at ultralow temperature in ultravacuum [J]. ***Infrared and Laser Engineering***, 2005, 34(1): 11-14. (in Chinese)

[7] Ho Y M, Parks H G, Vermeire B. A model for outgassing of organic contamination from wafer carrier boxes [C]// Advanced Semiconductor Manufacturing 2002 IEEE/SEMI Conference and Workshop. IEEE, 2002: 314-318.

[8] Wang Li, Sun Lichen, Yan Rongxin, et al. Outgassing analysis of testing products in unltra-high vacuum [J] ***Spacecraft Environment Engineering***, 2010, 27(6): 735-738.